

# Temporal Dynamics of Normalization Reweighting

Daniel H. Baker, Daniela Marinova, Richard Aveyard, Lydia J. Hargreaves, Alice Renton, Ruby Castellani, Phoebe Hall, Miriam Harmens, Georgia Holroyd, Beth Nicholson, Emily L. Williams, Hannah M. Hobson & Alex R. Wade

Department of Psychology, University of York, UK

## 1 Abstract

For decades, neural suppression in early visual cortex has been thought to be fixed. But recent work has challenged this assumption by showing that suppression can be *reweighted* based on recent history; when pairs of stimuli are repeatedly presented together, suppression between them strengthens. Here we investigate the temporal dynamics of this process using a steady-state visual evoked potential (SSVEP) paradigm that provides a time-resolved, direct index of suppression between pairs of stimuli flickering at different frequencies (5 and 7Hz). Our initial analysis of an existing EEG dataset (N=100) indicated that suppression increases substantially during the first 2-5 seconds of stimulus presentation (with some variation across stimulation frequency). We then collected new EEG data (N=100) replicating this finding for both monocular and dichoptic mask arrangements in a preregistered study designed to measure reweighting. A third experiment (N=20) used source localized MEG, and found that these effects are apparent in primary visual cortex (V1), consistent with results from neurophysiological work. Because long-standing theories propose inhibition/excitation differences in autism, we also compared reweighting between individuals with high vs low autistic traits, and with and without an autism diagnosis, across our 3 data sets (total N=220). We find no compelling differences in reweighting that are associated with autism. Our results support the normalization reweighting model, and indicate that for prolonged stimulation, increases in suppression occur on the order of 2-5 seconds after stimulus onset.

## 18 2 Introduction

Suppressive interactions between neurons are ubiquitous in the nervous system, with normalization considered a canonical neuronal computation (Carandini & Heeger, 2011). One consequence of normalization is that neurons tuned to different stimulus features modulate each others' firing, usually via a process of divisive suppression (Heeger, 1992). For decades the strength of suppression was treated as fixed, due to the observation that adapting to one stimulus does not decrease its suppressive potency (Foley & Chen, 1997; Freeman et al., 2002). This orthodoxy has been challenged by a series of innovative studies proposing

that normalization can be 'reweighted' by recent history (Aschner et al., 2018; Westrick et al., 2016; Yiltiz et al., 2020). When pairs of stimuli are repeatedly presented together, their neural representations appear to suppress each other more strongly. Far from being fixed, normalization may therefore be a dynamic process that is continuously updated by the sensory environment. Our objectives were to measure the time-course of changes in suppression non-invasively in the human brain, compare them across distinct anatomical pathways, and determine whether they differ as a function of autistic traits.

Plastic changes within the visual system occur over multiple timescales (see Webster, 2015 for a recent review). Cortical forms of adaptation to cues such as stimulus contrast (Blakemore & Campbell, 1969), orientation (Gibson & Radner, 1937) and motion (Mather et al., 2008) can be observed within a few seconds, but also build up over durations on the order of minutes (Greenlee et al., 1991). Other types of adaptation have been identified where changes occur over longer time periods, such as several hours (Kwon et al., 2009) or days (Haak et al., 2014). Previous normalization reweighting studies involved adapting sequences of

37 around 40 – 60s (Aschner et al., 2018; Yiltiz et al., 2020), but in principle reweighting might occur faster  
38 than this, consistent with other types of contrast adaptation.

39 Multiple suppressive pathways have been identified in the visual system, including between stimuli differing  
40 in orientation (Foley, 1994; Heeger, 1992), eye-of-origin (Dougherty et al., 2019; Legge, 1979; Sengpiel &  
41 Blakemore, 1994) and spatial position (Cannon & Fullenkamp, 1991; Petrov, 2005). At present there is  
42 evidence of normalization reweighting between stimuli with orthogonal orientations (Aschner et al., 2018),  
43 and adjacent spatial positions (Yiltiz et al., 2020). We anticipated that interocular suppression should also  
44 be subject to reweighting, but that there might be differences in the dynamics across suppressive pathways  
45 (Li et al., 2005; e.g. Meese & Baker, 2009; Sengpiel & Vorobyov, 2005). Comparing monocular and dichoptic  
46 suppression permits any contribution of early pre-cortical factors to be isolated. This is because interocular  
47 suppression is generally thought to impact in primary visual cortex (though see Dougherty et al., 2019), and  
48 bypasses any retinal and subcortical stages of processing that contribute to monocular suppression (Li et al.,  
49 2005).

50 Atypical sensory experience, including hypersensitivity to loud sounds, bright lights and strong odours or  
51 flavours, is widely reported by individuals on the autism spectrum (MacLennan et al., 2022; Simmons  
52 et al., 2009), but the causal mechanisms remain unclear. Fundamental measures of sensitivity including  
53 visual acuity (Tavassoli et al., 2011), contrast sensitivity (Koh et al., 2010), and audiometric performance  
54 (Rosenhall et al., 1999) are not consistently different from neurotypical controls. Theoretical accounts of  
55 sensory differences in autism have proposed that the balance of inhibition and excitation may be disrupted  
56 (Rosenberg et al., 2015; Rubenstein & Merzenich, 2003), yet the evidence is currently inconclusive (Sandhu et  
57 al., 2020; e.g. Schallmo et al., 2020; Van de Cruys et al., 2018). Our recent work identified an autism-related  
58 difference using steady-state EEG (Vilidaite et al., 2018), in which nonlinear (second harmonic) responses  
59 were weaker, implicating atypical suppression in autism.

60 Here we perform a time-course analysis of a previously published data set, and report two novel pre-registered  
61 experiments using EEG and MEG. Our data show that suppression increases substantially during the first 2–5  
62 seconds following stimulus onset, for both monocular and dichoptic masks. Source localisation of MEG data  
63 indicate that the reweighting is present as early as primary visual cortex (V1). We also hypothesised that  
64 normalization reweighting might differ as a function of autistic traits, but did not find convincing support  
65 for this hypothesis.

### 66 **3 Materials and Methods**

#### 67 **3.1 Participants**

68 Experiment 1 was completed by 100 adult participants (32 male, 68 female; mean age 21.9) in early 2015,  
69 and first reported by Vilidaite et al. (2018). Here we reanalysed the dataset, and report the results of  
70 masking conditions not previously published. Experiment 2 was completed by 100 adult participants (23  
71 male, 74 female, 3 other/not stated; mean age 22.1) in early 2022. Experiment 3 was completed by 10  
72 adults (2 male, 8 female) with a clinical diagnosis of autism, and 10 control participants who were closely  
73 matched for age (means of 21.8 and 22,  $t = 0.18$ ,  $df = 18$ ,  $p = 0.86$ ) and exactly matched for gender.  
74 Procedures in Experiments 1 and 2 were approved by the ethics committee of the Department of Psychology  
75 at the University of York. Procedures for Experiment 3 were approved by the ethics committee of the York  
76 Neuroimaging Centre. All participants provided written informed consent, and procedures were consistent  
77 with the Declaration of Helsinki.

#### 78 **3.2 Apparatus and stimuli**

79 In Experiments 1 and 2, stimuli were presented using a ViewPixx 3D LCD display device (VPixx Tech-  
80 nologies, Canada) with a resolution of 1920 × 1080 pixels and a refresh rate of 120Hz. The display was  
81 gamma corrected using a Minolta LS110 photometer. In Experiment 2, participants wore active stereo shut-  
82 ter glasses (Nvidia 3D Vision 2) that were synchronised with the display using an infra-red signal. EEG  
83 data were collected using a 64-channel Waveguard cap, and were amplified and digitised at 1000Hz using an

84 ANT Neuroscan system. Electrode impedance was maintained below  $5\text{k}\Omega$ , and referenced to a whole-head  
85 average.

86 In Experiment 3, stimuli were presented using a ProPixx DLP projector (VPixx Technologies) running at  
87 120Hz. Stereo presentation was enabled using a circular polariser that was synchronised with the projector  
88 refresh, and participants wore passive polarised glasses during the experiment. DLP projectors are perfectly  
89 linear, so gamma correction was not required. Data were acquired using a refurbished 248-channel 4D  
90 Neuroimaging Magnes 3600 MEG scanner, recording at 1001Hz. Participant head shape was digitised using  
91 a Polhemus Fastrak device, and head position was recorded at the start and end of each block by passing  
92 current through 5 position coils placed at fiducial points on the head. We also obtained structural MRI  
93 scans using a 3 Tesla Siemens Magnetom Prisma scanner to aid in source localisation. Two participants were  
94 not available for MRI scans, so we used the MNI ICBM152 template brain (Fonov et al., 2011) for these  
95 individuals.

96 Stimuli were patches of sine wave grating with a diameter of 2 degrees, flickering sinusoidally (on/off flicker)  
97 at either 5Hz or 7Hz. In Experiment 1 the gratings had a spatial frequency of 0.5c/deg, and in Experiments  
98 2 & 3 this was increased to 2c/deg. A symmetrical array of 36 individual patches tiled the display. In  
99 Experiment 1 the patch orientation was randomly selected on each trial, and all patches had the same  
100 orientation. In Experiments 2 & 3 each patch had a random orientation, which was intended to prevent any  
101 sequential effects between trials with similar orientations. The central patch was omitted and replaced by a  
102 fixation marker constructed from randomly overlaid squares. During each experiment, the fixation marker  
103 could be resampled on each trial with a probability of 0.5. Participants were instructed to monitor the  
104 fixation marker and count the number of times it changed throughout the experiment. This was intended  
105 to maintain attention towards the display and keep participants occupied.

106 Participants also completed either the short AQ (Hoekstra et al., 2011) in Experiment 1, or the full AQ  
107 (Baron-Cohen et al., 2001) in Experiments 2 and 3. For comparison across experiments, we rescaled the  
108 short AQ to the same range as the full AQ (0-50). In Experiments 2 and 3, the sensory perception quotient  
109 (SPQ) questionnaire (Tavassoli et al., 2014) was also completed.

### 110 3.3 Experimental design and statistical analysis

111 In Experiment 1, target stimuli flickering at 7Hz were presented at a range of contrasts (1 - 64%). In half  
112 of the conditions a superimposed orthogonal mask of 32% contrast was presented simultaneously, flickering  
113 at 5Hz. Stimuli were displayed for trials of 11 seconds, with a 3 second inter-trial interval. The experiment  
114 consisted of 4 blocks of trials, each lasting around 10 minutes, and resulting in 8 repetitions of each condition.  
115 Participants viewed the display from 57cm, were comfortably seated in an upright position, and were able to  
116 rest between blocks. Low latency 8-bit digital triggers transmitted the trial onset and condition information  
117 directly to the EEG amplifier.

118 The procedure for Experiment 2 was very similar, except that participants also wore stereo shutter glasses  
119 during the experiment. There were four conditions: (i) monocular presentation of a 5Hz stimulus of 48%  
120 contrast, (ii) monocular presentation of a 7Hz stimulus of 48% contrast, (iii) monocular presentation of  
121 both stimuli superimposed at right angles, and (iv) dichoptic presentation of both stimuli at right angles  
122 (i.e. one stimulus to the left eye, one to the right eye). Eye of presentation was pseudo-randomised to ensure  
123 equal numbers of left-eye and right-eye presentations. The trial duration was 6 seconds, with a 3 second  
124 inter-trial interval. Participants completed 3 blocks, each lasting around 10 minutes, resulting in a total of  
125 48 repetitions of each condition. Experiment 3 was identical, except that the projector screen was viewed  
126 from a distance of 85cm.

127 EEG data from Experiments 1 and 2 were first imported into Matlab using components of the EEGLab  
128 toolbox (Delorme & Makeig, 2004), and converted into a compressed ASCII format. Primary data analysis  
129 was then conducted using a bespoke *R* script. In brief, we epoched each trial and extracted the average  
130 timecourse across four occipital electrodes (*Oz*, *POz*, *O1* and *O2*), and then calculated the Fourier transform  
131 of this average waveform. We excluded trials for which the Mahalanobis distance of the complex Fourier  
132 components exceeded 3 (for details see Baker, 2021). This resulted in 0.25% of trials being excluded for  
133 Experiment 1, and 4.51% of trials for Experiment 2. Next we averaged the waveforms across all remaining

134 trials, and calculated the Fourier transform in a 1-second sliding window to generate timecourses for each  
135 participant. We divided the timecourse for the target-only condition by the timecourse for the target +  
136 mask condition to produce a suppression ratio. These were then converted to logarithmic (dB) units for  
137 averaging, calculation of standard errors, and statistical comparisons. For display purposes we smoothed the  
138 timecourses using a cubic spline function, however all statistical comparisons used the unsmoothed data.

139 Following the suggestion of a reviewer, we conducted an alternative fixed-phase analysis, where the signal  
140 in each 1 second epoch was multiplied by a sine wave of appropriate frequency and phase instead of taking  
141 the Fourier transform. The results were similar to our main analysis, and can be viewed in the Figures  
142 subdirectory of the project code repository (<https://github.com/bakerdh/normreweight/tree/main/Figures>). We also conducted simulations (also available in the code repository) to confirm that  
143 our analysis methods were not distorting the estimates of the suppression timecourse. In brief, although the  
144 1 second sliding time window does blur the signals in time, these effects are largely negated by calculating  
145 the suppression ratio because the blur cancels out across the numerator and denominator. Overall these  
146 simulations give us confidence in the accuracy of our estimates of suppression dynamics.  
147

148 For Experiment 3, we performed source localisation using a linearly constrained minimum variance (LCMV)  
149 beamformer algorithm, implemented in Brainstorm (Tadel et al., 2011). Structural MRI scans were processed  
150 using Freesurfer (Dale et al., 1999) to generate a 3D mesh of the head and brain, and we calculated source  
151 weights for each block with reference to a 5-minute empty room recording, usually recorded on the day of  
152 the experiment. The matrix of source weights for each block was used in a custom Matlab script to extract  
153 signals from V1, identified using the probabilistic maps of Wang et al. (2015). These signals were then  
154 imported into R for the main analysis, which was consistent with the EEG analysis described above. The  
155 outlier rejection procedure excluded 2.47% of trials for Experiment 3.

156 To make comparisons between groups of participants across time, we used a non-parametric cluster correction  
157 technique (Maris & Oostenveld, 2007) based on t-tests. Clusters were identified as temporally adjacent  
158 observations that were all statistically significant, and a summed t-value was calculated for each cluster.  
159 A null distribution was then generated by randomising group membership and recalculating the summed  
160 t-value for the largest cluster, and repeating this procedure 1000 times. Clusters were considered significant  
161 if they fell outside of the 95% confidence limits of the null distribution. We adapted this approach to test for  
162 significantly increasing suppression by conducting one-way t-tests between time points separated by 1000ms,  
163 and repeating the cluster correction procedure as described above.

### 164 **3.4 Preregistration, data and code accessibility**

165 Following a preliminary analysis of the data from Experiment 1, we preregistered our hypotheses and analysis  
166 plan for Experiments 2 and 3 on the Open Science Framework website. The preregistration document,  
167 along with raw and processed data, and analysis scripts, are publicly available at the project repository:  
168 <https://osf.io/ab3yv/>

## 169 **4 Results**

170 We began by reanalysing data from a steady-state visually evoked potential (SSVEP) experiment reported  
171 by Vilidaite et al. (2018). Participants viewed arrays of flickering gratings of varying contrasts. In some  
172 conditions a single grating orientation was present flickering at 7Hz (the target), whereas in other conditions  
173 a high contrast ‘mask’ was added at right angles to the target gratings, and flickering at 5Hz. The left  
174 panel of Figure 1a shows contrast response functions with and without the mask - the presence of the mask  
175 reduces the 7Hz response to the target (blue squares are below the black circles; significant main effect of  
176 mask contrast,  $F(1,99) = 26.52, p < 0.001$ ). Similarly, the right panel of Figure 1a shows that the 5Hz  
177 response to the mask was itself suppressed by the presence of high contrast targets (main effect of target  
178 contrast on the mask response,  $F(2.92,288.63) = 46.77, p < 0.001$ ; note that the data from the masking  
179 conditions were not reported by Vilidaite et al. (2018)). At both frequencies, responses were localised to the  
180 occipital pole (see insets).

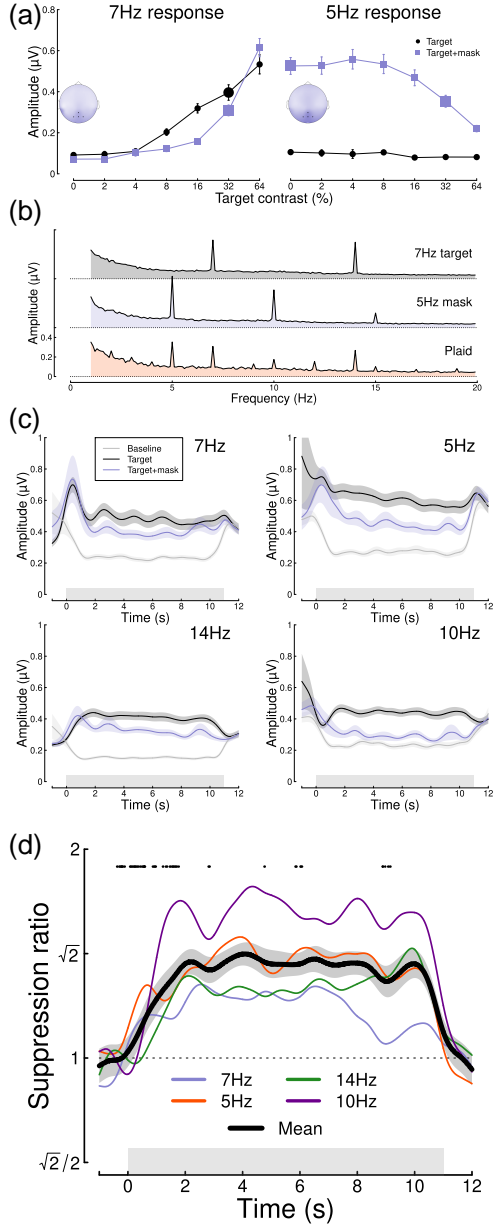


Figure 1: Summary of pilot analysis of data from Vilidiate et al. (2018). Panel (a) shows contrast response functions at the target frequency (7Hz, left) and the mask frequency (5Hz, right). Insets show the distribution of activity across the scalp, with points marking the electrodes over which signals were averaged (Oz, POz, O1 and O2). Panel (b) shows Fourier spectra for the single component stimuli and their combination (plaid). Note the strong second harmonic components at 14Hz and 10Hz. Panel (c) shows timecourses of frequency-locked responses to a single stimulus (black) and the plaid stimulus (blue), compared to a baseline condition (grey) where no stimulus was shown at the target frequency. Panel (d) shows the timecourse of suppression at each frequency (7Hz, 5Hz, 14Hz, 10Hz) and their average (black curve). Points around  $y = 1.8$  indicate a significantly increasing ratio (for the time window centred at each point). Error bars in panel (a) and shaded regions in panels (c,d) indicate  $\pm 1\text{SE}$  across  $N=100$  participants, and grey rectangles indicate the timing of stimulus presentation. The larger symbols in panel (a) indicate the conditions used for subsequent analyses.

181 We then performed a timecourse analysis, in which we analysed each 11-second trial using a sliding 1-second  
182 time window. The top panel of Figure 1c shows the response at the target frequency (7Hz) to a single  
183 stimulus of 32% contrast (black), and the response at 7Hz when the 32% contrast mask is added (blue).  
184 For comparison, a baseline timecourse is also shown (grey), which was the target response at 7Hz when a  
185 5Hz mask stimulus was shown (therefore controlling for attention, blinking etc.). Analogous responses are  
186 shown at three other frequencies - the mask frequency (5Hz), and the second harmonics of both target and  
187 mask frequencies (14Hz, 10Hz), at which strong responses were also found (see spectra in Figure 1b). The  
188 reduction in signal strength when a second component is added at a different orientation and frequency  
189 illustrates the masking effect. Surprisingly there was sometimes substantial activity before and after the  
190 stimulus was presented, as is especially clear in the baseline condition shown by the grey curves in Figure  
191 1c. We think the most likely explanation for this is broadband noise from participant movement during  
192 the breaks between trials. Since it is approximately equal across conditions it appears to cancel out in the  
193 suppression ratios (Figure 1d).

194 Taking the ratio of the two timecourses (the target only timecourse and the target timecourse when a mask  
195 was present) to calculate a masking index reveals that for 7Hz targets masking increases steeply during the  
196 first two seconds of stimulus presentation, and then plateaus for several seconds (blue trace in Figure 1d).  
197 A similar pattern is observed for the 5Hz mask (red trace in Figure 1d), as well as at the second harmonics,  
198 with some variability in the timecourse across frequencies; for example, at 5Hz suppression peaks at around  
199 4 seconds. The black trace shows the average masking ratio across all four frequencies, which rises steeply  
200 for just over two seconds and then stays approximately constant until stimulus offset. We conducted cluster-  
201 corrected t-tests between ratios separated by 1000ms, testing for an increase in suppression ratio across time  
202 (i.e. a one-sided test). Points at  $y = 1.8$  in Figure 1d indicate time points where the ratio is significantly  
203 increasing (i.e. there is significantly more suppression 500ms after the time point than there was 500ms before  
204 it), and occur up until 2.27 seconds after stimulus presentation. We also calculated an overall effect size by  
205 comparing the amount of suppression during the first 1000ms following stimulus onset with that between  
206 2000 and 3000ms, averaged across all temporal frequencies. This effect size (Cohen's  $d = 0.49$ ) indicated a  
207 medium-sized effect.

208 Our initial reanalysis was promising, however the data were noisy despite the large sample size (of  $N=100$ ),  
209 because each participant contributed only 8 trials (88 seconds) to each condition. We therefore preregistered  
210 two new experiments (see <https://osf.io/4qudc>) to investigate these effects in greater detail. These had a  
211 similar overall design to the Vilidaite et al. (2018) study, with some small changes intended to optimise  
212 the study (see Methods). The key differences were that we used shorter trials (because there were few  
213 changes in the latter part of the trials shown in Figure 1d), and also focussed all trials into a smaller  
214 number of conditions, such that each participant contributed 48 repetitions (288 seconds of data) to each of  
215 4 conditions.

216 Figure 2 summarises the results of our EEG experiment testing a further 100 adult participants. Averaged  
217 EEG waveforms showed a strong oscillatory component at each of the two stimulus flicker frequencies (Figure  
218 2a), which slightly lagged the driving signal. Signals were well-isolated in the Fourier domain (Figure 2b),  
219 and localised to occipital electrodes. Responses at 7Hz were weaker in the two masking conditions, showing  
220 significant changes in response amplitude for both the monocular ( $t = 7.56, df = 87, p < 0.001$ ) and dichoptic  
221 ( $t = 11.35, df = 87, p < 0.001$ ) masks. Dichoptic masking was significantly stronger than monocular masking  
222 ( $t = 7.96, df = 87, p < 0.001$ ), and a similar pattern was evident at 5Hz (note that for this experiment, the  
223 terms 'target' and 'mask' are arbitrary, as each component was presented at a single contrast).

224 The timecourse at both flicker frequencies showed an initial onset transient, and was then relatively stable  
225 for the 6 seconds of stimulus presentation (Figure 2c,d). The ratio of target only to target + mask conditions  
226 increased over time (Figure 2e,f) for both mask types. At 5Hz the increase in masking continued for as long  
227 as 5 seconds of stimulus presentation in the monocular condition (Figure 2e; points at  $y = 0.8$  indicate  
228 significantly increasing suppression, which continue until 5.1s (mon) or 4.2s (dich)), whereas at 7Hz the  
229 increase occurred primarily during the first 1.5 seconds after onset (Figure 2f; substantial clusters up to 1.5s  
230 (mon) and 1.7s (dich)). These differences across frequency are consistent with the pilot data (see Figure  
231 1d). Both monocular and dichoptic masks produced similar timecourses of suppression. We calculated an  
232 overall effect size comparing suppression in the first 1000ms after stimulus onset to the time window from

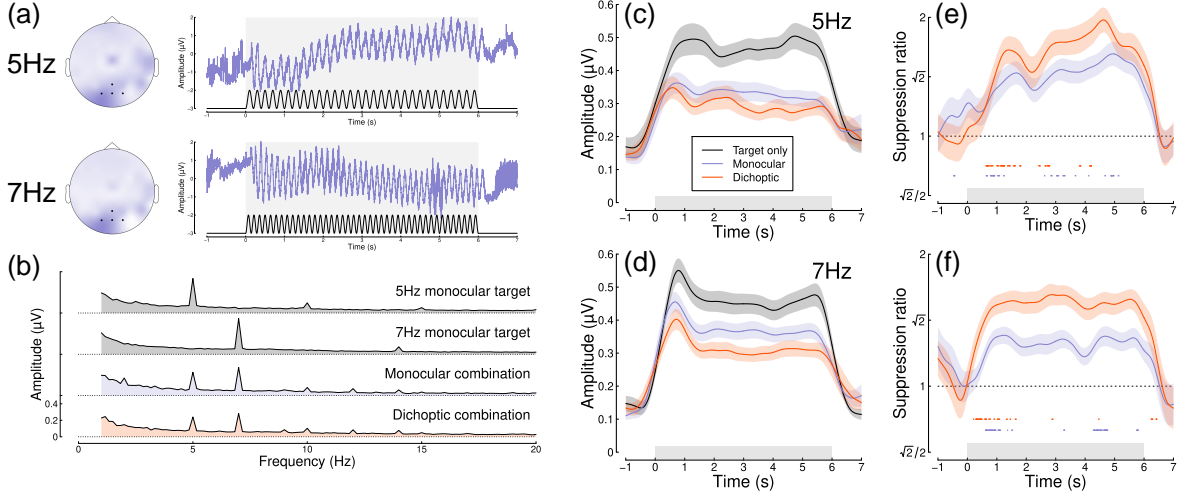


Figure 2: Summary of EEG results for  $N=100$  adult participants. Panel (a) shows scalp topographies and averaged waveforms for 5Hz (top) and 7Hz (bottom) stimuli. The black sine wave trace in each panel illustrates the driving contrast modulation, and black points on the scalp topographies indicate electrodes Oz, O1, O2 and POz. Panel (b) shows the Fourier amplitude spectrum for each condition, with clear peaks at 5Hz and 7Hz. Panels (c,d) show timecourses at each frequency for the target-only condition (black), and the monocular (blue) and dichoptic (red) masking conditions. Panels (e,f) show suppression ratios as a function of time for each mask type, with points around  $y = 0.8$  indicating a significantly increasing ratio. Shaded regions in panels (c-f) span  $\pm 1\text{SE}$  across participants, and light grey rectangles indicate the period of stimulus presentation.

3000-4000ms, pooling over frequency and mask type. This had a value of  $d = 0.33$ . Overall, this second study confirmed that normalization increases during the first few seconds of a steady-state trial, and extends this finding to dichoptic mask arrangements.

Next we repeated the experiment on 20 participants using a 248-channel whole-head cryogenic MEG system. Half of the participants had a diagnosis of autism, and the remainder were age- and gender-matched controls. Source localisation using a linearly constrained minimum variance (LCMV) beamformer algorithm (Van Veen et al., 1997) showed strong localisation of steady-state signals at the occipital pole (see Figure 3a), and in the Fourier domain (Figure 3b). Responses from the most responsive V1 vertex showed a similar timecourse to those of the EEG experiments at both frequencies (Figure 3c,d), and showed increasing suppression during the first few seconds of stimulus presentation (Figure 3e,f). The normalization reweighting effect was again clearest at 5Hz, especially for the dichoptic condition (red curve in Figure 3e), which increased until 2.5s. This confirms that the reweighting effects can occur as early as primary visual cortex, consistent with findings from neurophysiology (Aschner et al., 2018). However the data are more variable than for our EEG experiments, and had fewer significant clusters, perhaps owing to a power reduction caused by the smaller sample size for this dataset and greater heterogeneity across frequency. When pooling effects over frequency and condition, the overall effect size ( $d = 0.03$ ) was near zero.

Intermodulation responses, at sums and differences of different stimulation frequencies, are another marker of nonlinear interaction (Cunningham et al., 2017; Regan & Regan, 1988; Tsai et al., 2012). We also calculated the timecourse of the sum intermodulation terms (at 12Hz) in our data sets (the difference terms at 2Hz were negligible). Figure 4 shows that for both EEG experiments, the intermodulation term increases during the first 1 second of stimulus presentation and then remains approximately constant. The intermodulation response in the MEG data was less clear, consistent with the spectra shown in Figure 3b. It seems unlikely that intermodulation terms are useful for monitoring the timecourse of normalization reweighting, and indeed they may derive from a nonlinear process other than suppression, such as exponentiation and signal combination (Regan & Regan, 1988). Previous work has identified situations in which suppression is constant, but the intermodulation term changes substantially between conditions depending on the extent

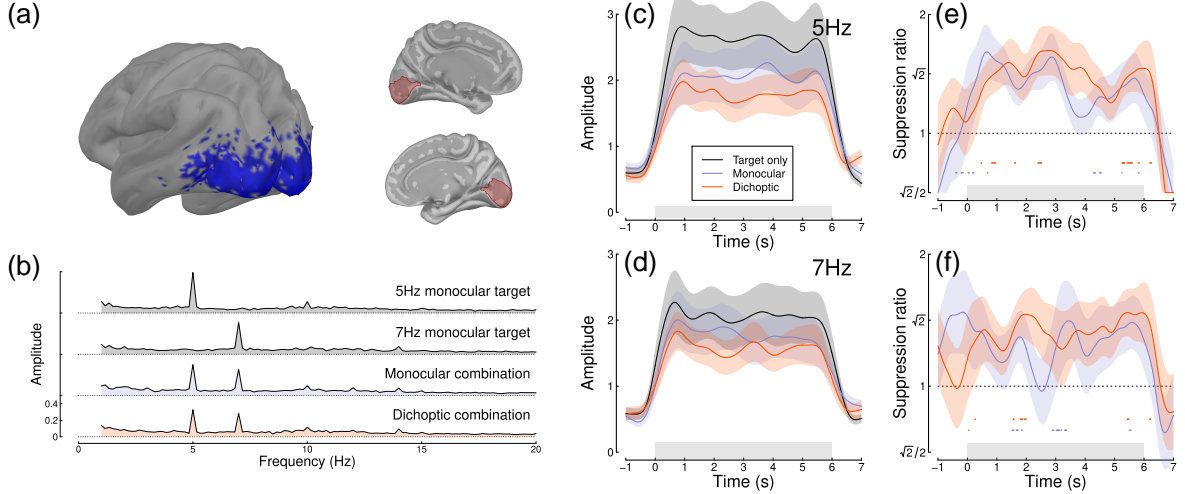


Figure 3: Summary of MEG results for  $N=20$  adults. Panel (a) shows average SSVEP response in source space, thresholded at  $\text{SNR}=2$  (blue, left), and locations of the V1 ROI on the medial surface of both hemispheres (right, red). Panel (b) shows the Fourier spectra for the four experimental conditions, from the most responsive vertex in V1. Panels (c,d) show timecourses at 5Hz and 7Hz, and panels (e,f) show suppression ratios for the monocular and dichoptic conditions at each frequency, with points around  $y = 0.8$  indicating a significantly increasing ratio. Shaded regions in panels (c-f) indicate  $\pm 1\text{SE}$  across participants, and light grey rectangles indicate the period of stimulus presentation.

259 of signal pooling (Cunningham et al., 2017).

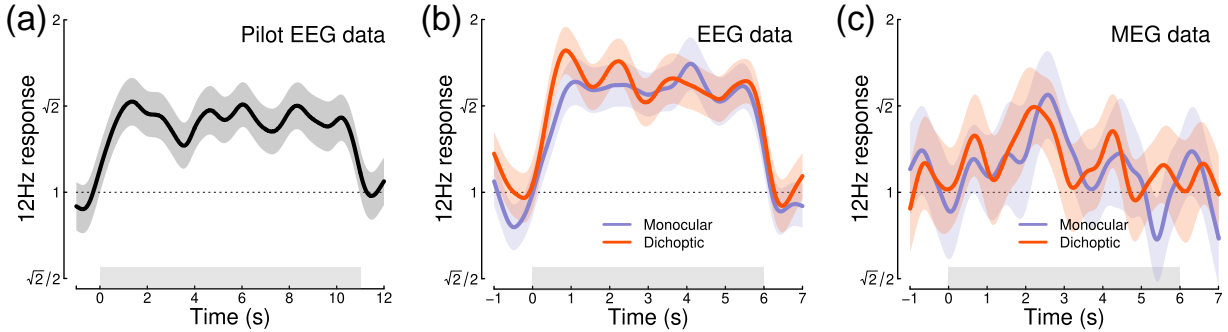


Figure 4: Timecourse of the sum intermodulation term at 12Hz across three experiments. In both EEG experiments, the intermodulation response increases during the first 1 second of stimulus presentation. Responses are calculated as a proportional increase relative to the target-only conditions (where the intermodulation response is absent), for direct comparison with the suppression ratios in Figures 1-3. Shaded regions indicate  $\pm 1\text{SE}$ .

260 To investigate whether normalization reweighting effects differ with respect to autistic traits, we then split  
 261 each dataset (averaged across temporal frequency) using median AQ score (for the EEG experiments) or  
 262 according to diagnostic group (autism vs controls) for the MEG data. Figure 5a-c shows distributions of AQ  
 263 scores for each experiment, and indicates for the pilot and EEG data which participants were in the high  
 264 (purple) and low (green) AQ groups. The median AQ scores were 14 for the pilot data, and 18 for the EEG  
 265 data. In the MEG experiment, AQ scores for the autism group (mean 36.1) and the control group (mean  
 266 16.7) were significantly different ( $t = 6.00$ ,  $df = 14.2$ ,  $p < 0.001$ ), with minimal overlap (one participant  
 267 with an autism diagnosis had an AQ score marginally lower than the highest AQ scores from the control  
 268 group). These distributions are consistent with previous results for AQ (Baron-Cohen et al., 2001).

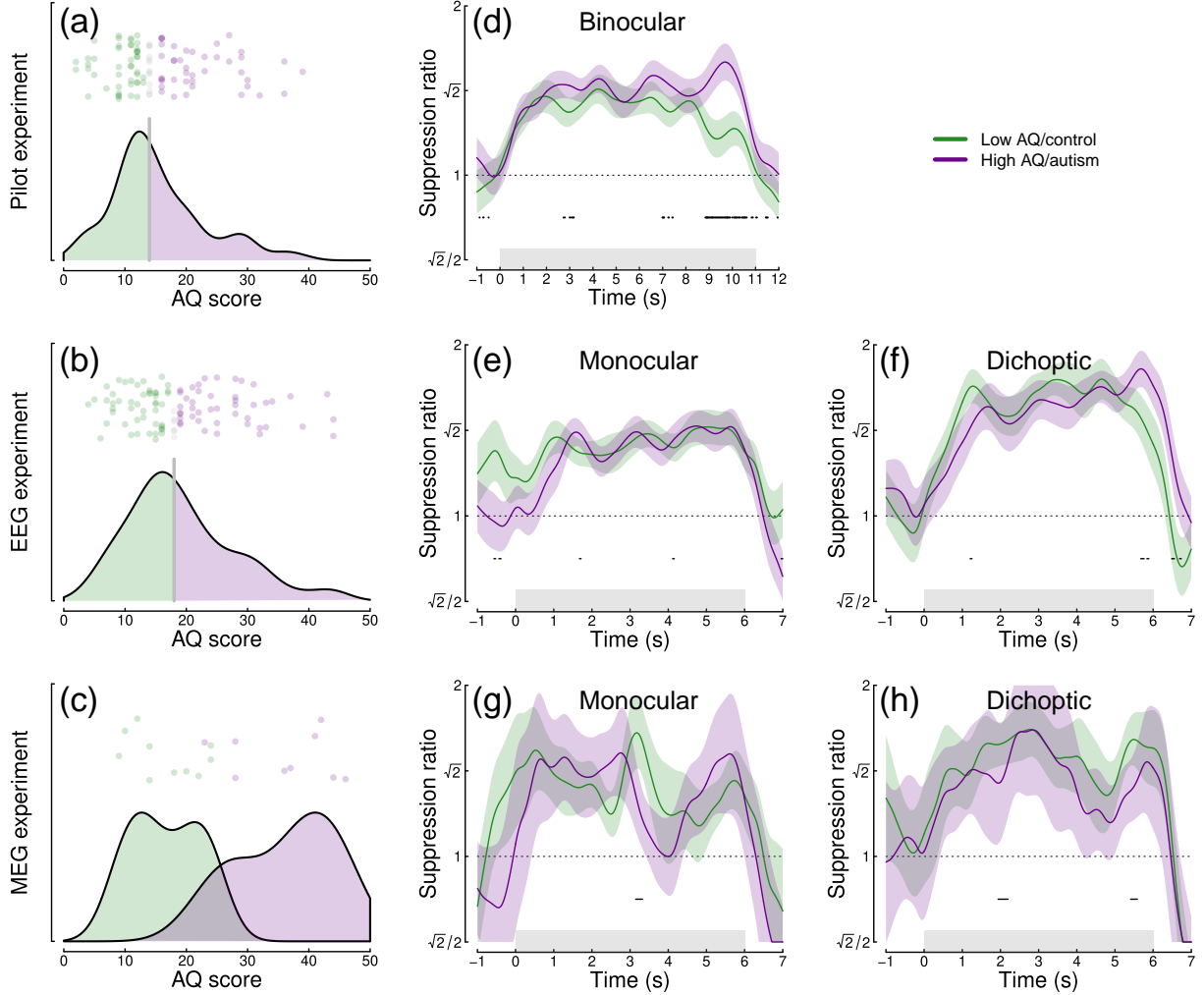


Figure 5: Analysis of the effect of autistic traits on normalization reweighting. Panels (a-c) show distributions of AQ scores across the three data sets. Panels (d-h) show timecourses of suppression averaged across stimulation frequency, and split by AQ score (d-f) or autism status (g, h). Panels (d,e,g) are for binocular or monocular presentation, and panels (f,h) are for dichoptic presentation. Shaded regions in panels (d-h) indicate  $\pm 1\text{SE}$  across participants, and black points at  $y = 0.8$  indicate significant differences between groups.

269 We compared the timecourse of suppression between groups using a nonparametric cluster correction ap-  
270 proach (Maris & Oostenveld, 2007) to control the type I error rate. Significant clusters are indicated at  $y =$   
271 0.8 in panels d-h of Figure 5. Despite some occasionally significant clusters, there is no clear or consistent  
272 difference between groups across our three data sets. In particular, none of the significant clusters occur  
273 during the first few seconds of stimulus onset, when reweighting takes place. We also compared suppression  
274 ratios calculated on Fourier components for the full trial, and found no significant effects of autism on sup-  
275 pression strength. For Experiment 1 we assessed the first and second harmonics separately, but also found  
276 no AQ-related differences. We therefore conclude that autism/AQ score is not associated with normalization  
277 reweighting, or the strength of suppression more generally.

## 278 5 Discussion

279 We found evidence of dynamic normalization reweighting across three separate datasets. Suppression in-  
280 creased significantly during the first 2-5 seconds of stimulus presentation, though with some variation across  
281 temporal frequency. Relative to the first 1 second of stimulus presentation, the increase in suppression after  
282 3 seconds constituted an effect size of  $d = 0.49$  for the pilot data,  $d = 0.33$  for our new EEG experiment,  
283 and  $d = 0.03$  for our MEG experiment (pooled across temporal frequency and monocular and dichoptic  
284 conditions). Reweighting had a similar timecourse for monocular and dichoptic stimulus presentation, and  
285 was apparent as early as V1. We did not find compelling differences associated with autism, or high vs  
286 low autistic traits. In the remainder of this section we will discuss possible explanations for temporal fre-  
287 quency differences, evidence for inhibitory differences in autism, and more general implications of dynamic  
288 normalization reweighting.

289 One important question is whether the dynamic increase in suppression can be explained by the stimulus  
290 onset transient. This is a possibility that cannot be ruled out for some of our data. For example, the steep  
291 increase in suppression in Figure 2f has a similar timecourse to the onset transient in Figure 2d. However,  
292 there are also counterexamples where suppression continues to increase well beyond the first 1 second of  
293 stimulus presentation (e.g. Figure 2e). It is currently unclear why there appear to be such substantial  
294 differences between temporal frequency conditions, especially with such similar frequencies (5 and 7Hz).  
295 However the differences are relatively consistent across experiments. For example, 5Hz flicker produces a  
296 more gradual increase in suppression across all three data sets, compared with 7Hz flicker. These differences  
297 may be a consequence of visual channels with different temporal tuning interacting with the stimulation  
298 frequency, as well as any nonlinearities that govern suppression. Or there could be an asymmetry, whereby  
299 the relative temporal frequency between the two stimulus components affects the character of suppression  
300 (Liza & Ray, 2022). We hope to be able to model these effects in the future, for example by using dynamic  
301 models of early vision that incorporate time-lagged gain control (e.g. Zhou et al., 2019).

302 We did not observe clear differences in the timecourse between monocular and dichoptic suppression. This is  
303 important, because the dichoptic arrangement bypasses early stages of processing before the cortex (e.g. the  
304 retina and lateral geniculate nucleus). It suggests that the dynamic increases in suppression occur in the  
305 cortex, consistent with our MEG data that find evidence of reweighting in V1 (see Fig 3), and with previous  
306 neurophysiological work (Aschner et al., 2018). It is currently unclear whether these effects originate in  
307 V1, or might involve feedback from higher areas. The similarity between monocular and dichoptic effects  
308 also differs from work on adaptation to individual mask components. In both physiological (Li et al., 2005;  
309 Sengpiel & Vorobyov, 2005) and psychophysical (Baker et al., 2007) paradigms, adapting to a dichoptic mask  
310 reduces its potency, whereas adapting to a monocular mask has little or no effect. Normalization reweighting  
311 offers an explanation for why monocular masks presented in isolation do not adapt: if suppressive weights  
312 are determined by co-occurrence of stimuli, presentation of an isolated mask will have little effect. However  
313 this cannot explain the dichoptic adaptation effects without invoking additional binocular processes, such as  
314 competition between summing and differencing channels (e.g. May et al., 2012).

315 The relationship between normalization reweighting and other forms of visual plasticity and adaptation is  
316 currently unclear. One phenomenon that might be closely related to our dichoptic effect is the change in  
317 interocular suppression that occurs when one eye is patched for a period of time (Lunghi et al., 2011). In  
318 the patching paradigm, the inputs to the two eyes are uncorrelated while one eye is patched, which the

normalization reweighting model predicts should reduce suppression between the eyes. Most studies using patching have focussed on the resulting imbalance between the patched and non-patched eye, in which the patched eye contributes more to binocular single vision than the non-patched eye. In principle this could be due to increased suppression of the non-patched eye (inconsistent with normalization reweighting), or reduced suppression of the patched eye (consistent with normalization reweighting). It is difficult to distinguish these possibilities using paradigms that assess the balance between the two eyes, such as the binocular rivalry paradigm from the original Lunghi et al. (2011) study. However subsequent work has shown that patching increases the patched eye's response (Zhou et al., 2015), and reduces both dichoptic masking (Baldwin & Hess, 2018) and levels of the inhibitory neurotransmitter GABA (Lunghi et al., 2015). All of these findings are consistent with a reweighting account.

Autism is composed of a set of heterogenous symptoms and characteristics, and normalization reweighting may have a more specific relationship to some aspects of autism, rather than autism per se. For this reason, we also examined relationships with the sensory perception quotient (SPQ) to examine whether sensory experiences specifically were related to normalization reweighting. SPQ scores showed significant negative correlation with AQ for the data sets from Experiments 2 and 3 (EEG data,  $r = -0.35$ ,  $p < 0.001$ ; MEG data,  $r = -0.57$ ,  $p = 0.011$ ) with effect sizes comparable to those reported previously (Tavassoli et al., 2014). We also conducted an exploratory analysis of the EEG data from Experiment 2, splitting participants by SPQ instead of AQ. However this analysis did not reveal any convincing differences in normalization reweighting either. Our preregistration also proposed to replicate our earlier finding of a reduced second harmonic response in participants with autism/high AQ scores. However the changes to the experimental design greatly reduced the second harmonic response in both experiments, such that it could not be observed reliably (see Figures 2b and 3b). We were therefore not confident in conducting this analysis. We suspect that the increase in spatial frequency from 0.5 c/deg in the Vilidaite et al. (2018) study to 2 c/deg here is most likely responsible for the dramatically reduced second harmonic response.

The idea that the dynamic balance of inhibition and excitation might be different in autism (Rosenberg et al., 2015; Rubenstein & Merzenich, 2003) has compelling face validity. For example, individuals with autism often report difficulties with changes in their sensory environment, which might be due to gain control processes failing to adapt appropriately. Indeed, there is experimental evidence of reduced adaptation across various domains (Pellicano et al., 2007; Turi et al., 2015), which is predicted by some autism models (Pellicano & Burr, 2012). However this appears not to extend to changes in normalization reweighting, despite the link between reweighting and adaptation (Westrick et al., 2016).

## 5.1 Conclusions

We investigated the timecourse of normalization reweighting across three datasets, with a total of 220 participants. We found clear evidence that suppression increases during the first 2-5 seconds of stimulus presentation, though there were differences across frequency that are currently unexplained. We did not find evidence of autism-related differences in either the magnitude or timecourse of suppression. Our results support an emerging theory that suppression is a dynamic process that allows sensory systems to recalibrate according to their recent history.

## 6 Acknowledgements

Supported by BBSRC grant BB/V007580/1 awarded to DHB and ARW. We are grateful to all of the participants who took part in the experiments reported here.

## References

- Aschner, A., Solomon, S. G., Landy, M. S., Heeger, D. J., & Kohn, A. (2018). Temporal contingencies determine whether adaptation strengthens or weakens normalization. *J Neurosci*, 38(47), 10129–10142. <https://doi.org/10.1523/JNEUROSCI.1131-18.2018>
- Baker, D. H. (2021). Statistical analysis of periodic data in neuroscience. *Neurons, Behavior, Data Analysis, and Theory*, 5(3). <https://doi.org/10.51628/001c.27680>

- 366 Baker, D. H., Meese, T. S., & Summers, R. J. (2007). Psychophysical evidence for two routes to suppression  
367 before binocular summation of signals in human vision. *Neuroscience*, 146(1), 435–448. <https://doi.org/10.1016/j.neuroscience.2007.01.030>
- 368 Baldwin, A. S., & Hess, R. F. (2018). The mechanism of short-term monocular deprivation is not simple:  
369 Separate effects on parallel and cross-oriented dichoptic masking. *Sci Rep*, 8(1), 6191. <https://doi.org/10.1038/s41598-018-24584-9>
- 370 Baron-Cohen, S., Wheelwright, S., Skinner, R., Martin, J., & Clubley, E. (2001). The autism-spectrum  
371 quotient (AQ): Evidence from asperger syndrome/high-functioning autism, males and females, scientists  
372 and mathematicians. *J Autism Dev Disord*, 31(1), 5–17. <https://doi.org/10.1023/a:1005653411471>
- 373 Blakemore, C., & Campbell, F. W. (1969). On the existence of neurones in the human visual system  
374 selectively sensitive to the orientation and size of retinal images. *J Physiol*, 203(1), 237–260. <https://doi.org/10.1113/jphysiol.1969.sp008862>
- 375 Cannon, M. W., & Fullenkamp, S. C. (1991). Spatial interactions in apparent contrast: Inhibitory effects  
376 among grating patterns of different spatial frequencies, spatial positions and orientations. *Vision Res*,  
377 31(11), 1985–1998. [https://doi.org/10.1016/0042-6989\(91\)90193-9](https://doi.org/10.1016/0042-6989(91)90193-9)
- 378 Carandini, M., & Heeger, D. J. (2011). Normalization as a canonical neural computation. *Nature Reviews  
379 Neuroscience*, 13(1), 51–62. <https://doi.org/10.1038/nrn3136>
- 380 Cunningham, D. G. M., Baker, D. H., & Peirce, J. W. (2017). Measuring nonlinear signal combination using  
381 EEG. *J Vis*, 17(5), 10. <https://doi.org/10.1167/17.5.10>
- 382 Dale, A. M., Fischl, B., & Sereno, M. I. (1999). Cortical surface-based analysis. I. Segmentation and surface  
383 reconstruction. *Neuroimage*, 9(2), 179–194. <https://doi.org/10.1006/nimg.1998.0395>
- 384 Delorme, A., & Makeig, S. (2004). EEGLAB: An open source toolbox for analysis of single-trial EEG  
385 dynamics including independent component analysis. *J Neurosci Methods*, 134(1), 9–21. <https://doi.org/10.1016/j.jneumeth.2003.10.009>
- 386 Dougherty, K., Schmid, M. C., & Maier, A. (2019). Binocular response modulation in the lateral geniculate  
387 nucleus. *J Comp Neurol*, 527(3), 522–534. <https://doi.org/10.1002/cne.24417>
- 388 Foley, J. M. (1994). Human luminance pattern-vision mechanisms: Masking experiments require a new  
389 model. *J Opt Soc Am A Opt Image Sci Vis*, 11(6), 1710–1719. <https://doi.org/10.1364/josaa.11.001710>
- 390 Foley, J. M., & Chen, C. C. (1997). Analysis of the effect of pattern adaptation on pattern pedestal effects:  
391 A two-process model. *Vision Res*, 37(19), 2779–2788. [https://doi.org/10.1016/s0042-6989\(97\)00081-3](https://doi.org/10.1016/s0042-6989(97)00081-3)
- 392 Fonov, V., Evans, A. C., Botteron, K., Almli, C. R., McKinstry, R. C., Collins, D. L., & Brain Development  
393 Cooperative Group. (2011). Unbiased average age-appropriate atlases for pediatric studies. *Neuroimage*,  
394 54(1), 313–327. <https://doi.org/10.1016/j.neuroimage.2010.07.033>
- 395 Freeman, T. C. B., Durand, S., Kiper, D. C., & Carandini, M. (2002). Suppression without inhibition in  
396 visual cortex. *Neuron*, 35(4), 759–771. [https://doi.org/10.1016/s0896-6273\(02\)00819-x](https://doi.org/10.1016/s0896-6273(02)00819-x)
- 397 Gibson, J. J., & Radner, M. (1937). Adaptation, after-effect and contrast in the perception of tilted lines.  
398 I. Quantitative studies. *Journal of Experimental Psychology*, 20(5), 453–467. <https://doi.org/10.1037/h0059826>
- 399 Greenlee, M. W., Georgeson, M. A., Magnussen, S., & Harris, J. P. (1991). The time course of adaptation  
400 to spatial contrast. *Vision Res*, 31(2), 223–236. [https://doi.org/10.1016/0042-6989\(91\)90113-j](https://doi.org/10.1016/0042-6989(91)90113-j)
- 401 Haak, K. V., Fast, E., Bao, M., Lee, M., & Engel, S. A. (2014). Four days of visual contrast deprivation  
402 reveals limits of neuronal adaptation. *Curr Biol*, 24(21), 2575–2579. <https://doi.org/10.1016/j.cub.2014.09.027>
- 403 Heeger, D. J. (1992). Normalization of cell responses in cat striate cortex. *Vis Neurosci*, 9(2), 181–197.  
404 <https://doi.org/10.1017/s0952523800009640>
- 405 Hoekstra, R. A., Vinkhuyzen, A. A. E., Wheelwright, S., Bartels, M., Boomsma, D. I., Baron-Cohen, S.,  
406 Posthuma, D., & Sluis, S. van der. (2011). The construction and validation of an abridged version of the  
407 autism-spectrum quotient (AQ-short). *J Autism Dev Disord*, 41(5), 589–596. <https://doi.org/10.1007/s10803-010-1073-0>
- 408 Koh, H. C., Milne, E., & Dobkins, K. (2010). Spatial contrast sensitivity in adolescents with autism spectrum  
409 disorders. *J Autism Dev Disord*, 40(8), 978–987. <https://doi.org/10.1007/s10803-010-0953-7>
- 410 Kwon, M., Legge, G. E., Fang, F., Cheong, A. M. Y., & He, S. (2009). Adaptive changes in visual cortex  
411 following prolonged contrast reduction. *J Vis*, 9(2), 20.1–16. <https://doi.org/10.1167/9.2.20>
- 412 Legge, G. E. (1979). Spatial frequency masking in human vision: Binocular interactions. *J Opt Soc Am*,

- 420 69(6), 838–847. <https://doi.org/10.1364/josa.69.000838>
- 421 Li, B., Peterson, M. R., Thompson, J. K., Duong, T., & Freeman, R. D. (2005). Cross-orientation  
422 suppression: Monoptic and dichoptic mechanisms are different. *J Neurophysiol*, 94(2), 1645–1650.  
423 <https://doi.org/10.1152/jn.00203.2005>
- 424 Liza, K., & Ray, S. (2022). Local interactions between steady-state visually evoked potentials at nearby  
425 flickering frequencies. *J Neurosci*, 42(19), 3965–3974. <https://doi.org/10.1523/JNEUROSCI.0180-22.2022>
- 426 Lunghi, C., Burr, D. C., & Morrone, C. (2011). Brief periods of monocular deprivation disrupt ocular balance  
427 in human adult visual cortex. *Curr Biol*, 21(14), R538–9. <https://doi.org/10.1016/j.cub.2011.06.004>
- 428 Lunghi, C., Emir, U. E., Morrone, M. C., & Bridge, H. (2015). Short-term monocular deprivation alters  
429 GABA in the adult human visual cortex. *Curr Biol*, 25(11), 1496–1501. <https://doi.org/10.1016/j.cub.2015.04.021>
- 430 MacLennan, K., O'Brien, S., & Tavassoli, T. (2022). In our own words: The complex sensory experiences of  
431 autistic adults. *J Autism Dev Disord*, 52(7), 3061–3075. <https://doi.org/10.1007/s10803-021-05186-3>
- 432 Maris, E., & Oostenveld, R. (2007). Nonparametric statistical testing of EEG- and MEG-data. *J Neurosci  
Methods*, 164(1), 177–190. <https://doi.org/10.1016/j.jneumeth.2007.03.024>
- 433 Mather, G., Pavan, A., Campana, G., & Casco, C. (2008). The motion aftereffect reloaded. *Trends Cogn  
Sci*, 12(12), 481–487. <https://doi.org/10.1016/j.tics.2008.09.002>
- 434 May, K. A., Zhaoping, L., & Hibbard, P. B. (2012). Perceived direction of motion determined by adaptation  
435 to static binocular images. *Curr Biol*, 22(1), 28–32. <https://doi.org/10.1016/j.cub.2011.11.025>
- 436 Meese, T. S., & Baker, D. H. (2009). Cross-orientation masking is speed invariant between ocular pathways  
437 but speed dependent within them. *Journal of Vision*, 9(5), 2. <https://doi.org/10.1167/9.5.2>
- 438 Pellicano, E., & Burr, D. (2012). When the world becomes 'too real': A bayesian explanation of autistic  
439 perception. *Trends Cogn Sci*, 16(10), 504–510. <https://doi.org/10.1016/j.tics.2012.08.009>
- 440 Pellicano, E., Jeffery, L., Burr, D., & Rhodes, G. (2007). Abnormal adaptive face-coding mechanisms in  
441 children with autism spectrum disorder. *Curr Biol*, 17(17), 1508–1512. <https://doi.org/10.1016/j.cub.2007.07.065>
- 442 Petrov, Y. (2005). Two distinct mechanisms of suppression in human vision. *Journal of Neuroscience*,  
443 25(38), 8704–8707. <https://doi.org/10.1523/jneurosci.2871-05.2005>
- 444 Regan, M. P., & Regan, D. (1988). A frequency domain technique for characterizing nonlinearities in  
445 biological systems. *Journal of Theoretical Biology*, 133(3), 293–317. [https://doi.org/https://doi.org/10.1016/S0022-5193\(88\)80323-0](https://doi.org/https://doi.org/10.1016/S0022-5193(88)80323-0)
- 446 Rosenberg, A., Patterson, J. S., & Angelaki, D. E. (2015). A computational perspective on autism. *Proc  
Natl Acad Sci U S A*, 112(30), 9158–9165. <https://doi.org/10.1073/pnas.1510583112>
- 447 Rosenhall, U., Nordin, V., Sandström, M., Ahlsén, G., & Gillberg, C. (1999). Autism and hearing loss. *J  
Autism Dev Disord*, 29(5), 349–357. <https://doi.org/10.1023/a:1023022709710>
- 448 Rubenstein, J. L. R., & Merzenich, M. M. (2003). Model of autism: Increased ratio of excitation/inhibition  
449 in key neural systems. *Genes Brain Behav*, 2(5), 255–267. <https://doi.org/10.1034/j.1601-183x.2003.00037.x>
- 450 Sandhu, T. R., Reese, G., & Lawson, R. P. (2020). Preserved low-level visual gain control in autistic adults.  
451 *Wellcome Open Research*, 4(208). <https://doi.org/10.12688/wellcomeopenres.15615.1>
- 452 Schallmo, M.-P., Kolodny, T., Kale, A. M., Millin, R., Flevaris, A. V., Edden, R. A. E., Gerdts, J., Bernier,  
453 R. A., & Murray, S. O. (2020). Weaker neural suppression in autism. *Nat Commun*, 11(1), 2675.  
454 <https://doi.org/10.1038/s41467-020-16495-z>
- 455 Sengpiel, F., & Blakemore, C. (1994). Interocular control of neuronal responsiveness in cat visual cortex.  
456 *Nature*, 368(6474), 847–850. <https://doi.org/10.1038/368847a0>
- 457 Sengpiel, F., & Vorobyov, V. (2005). Intracortical origins of interocular suppression in the visual cortex. *J  
Neurosci*, 25(27), 6394–6400. <https://doi.org/10.1523/JNEUROSCI.0862-05.2005>
- 458 Simmons, D. R., Robertson, A. E., McKay, L. S., Toal, E., McAleer, P., & Pollick, F. E. (2009). Vision in  
459 autism spectrum disorders. *Vision Research*, 49(22), 2705–2739. <https://doi.org/10.1016/j.visres.2009.08.005>
- 460 Tadel, F., Baillet, S., Mosher, J. C., Pantazis, D., & Leahy, R. M. (2011). Brainstorm: A user-friendly  
461 application for MEG/EEG analysis. *Comput Intell Neurosci*, 2011, 879716. <https://doi.org/10.1155/2011/879716>

- 474 Tavassoli, T., Hoekstra, R. A., & Baron-Cohen, S. (2014). The sensory perception quotient (SPQ): Development and validation of a new sensory questionnaire for adults with and without autism. *Mol Autism*, 5, 29. <https://doi.org/10.1186/2040-2392-5-29>
- 475
- 476
- 477 Tavassoli, T., Latham, K., Bach, M., Dakin, S. C., & Baron-Cohen, S. (2011). Psychophysical measures of visual acuity in autism spectrum conditions. *Vision Research*, 51(15), 1778–1780. <https://doi.org/10.1016/j.visres.2011.06.004>
- 478
- 479
- 480 Tsai, J. J., Wade, A. R., & Norcia, A. M. (2012). Dynamics of normalization underlying masking in human visual cortex. *J Neurosci*, 32(8), 2783–2789. <https://doi.org/10.1523/JNEUROSCI.4485-11.2012>
- 481
- 482 Turi, M., Burr, D. C., Igliozi, R., Aagten-Murphy, D., Muratori, F., & Pellicano, E. (2015). Children with autism spectrum disorder show reduced adaptation to number. *Proc Natl Acad Sci U S A*, 112(25), 7868–7872. <https://doi.org/10.1073/pnas.1504099112>
- 483
- 484
- 485 Van de Cruys, S., Vanmarcke, S., Steyaert, J., & Wagemans, J. (2018). Intact perceptual bias in autism contradicts the decreased normalization model. *Scientific Reports*, 8(1). <https://doi.org/10.1038/s41598-018-31042-z>
- 486
- 487
- 488 Van Veen, B. D., Drongelen, W. van, Yuchtman, M., & Suzuki, A. (1997). Localization of brain electrical activity via linearly constrained minimum variance spatial filtering. *IEEE Trans Biomed Eng*, 44(9), 867–880. <https://doi.org/10.1109/10.623056>
- 489
- 490
- 491 Vilidaite, G., Norcia, A. M., West, R. J. H., Elliott, C. J. H., Pei, F., Wade, A. R., & Baker, D. H. (2018). Autism sensory dysfunction in an evolutionarily conserved system. *Proc Biol Sci*, 285(1893), 20182255. <https://doi.org/10.1098/rspb.2018.2255>
- 492
- 493
- 494 Wang, L., Mruczek, R. E. B., Arcaro, M. J., & Kastner, S. (2015). Probabilistic maps of visual topography in human cortex. *Cereb Cortex*, 25(10), 3911–3931. <https://doi.org/10.1093/cercor/bhu277>
- 495
- 496 Webster, M. A. (2015). Visual adaptation. *Annu Rev Vis Sci*, 1, 547–567. <https://doi.org/10.1146/annurev-vision-082114-035509>
- 497
- 498 Westrick, Z. M., Heeger, D. J., & Landy, M. S. (2016). Pattern adaptation and normalization reweighting. *Journal of Neuroscience*, 36(38), 9805–9816. <https://doi.org/10.1523/jneurosci.1067-16.2016>
- 499
- 500 Yiltiz, H., Heeger, D. J., & Landy, M. S. (2020). Contingent adaptation in masking and surround suppression. *Vision Res*, 166, 72–80. <https://doi.org/10.1016/j.visres.2019.11.004>
- 501
- 502 Zhou, J., Baker, D. H., Simard, M., Saint-Amour, D., & Hess, R. F. (2015). Short-term monocular patching boosts the patched eye's response in visual cortex. *Restor Neurol Neurosci*, 33(3), 381–387. <https://doi.org/10.3233/RNN-140472>
- 503
- 504
- 505 Zhou, J., Benson, N. C., Kay, K., & Winawer, J. (2019). Predicting neuronal dynamics with a delayed gain control model. *PLoS Comput Biol*, 15(11), e1007484. <https://doi.org/10.1371/journal.pcbi.1007484>
- 506